Korean J. Chem. Eng., **31**(6), 1002-1007 (2014)
DOI: 10.1007/s11814-014-0035-1

pISSN: 0256-1115
eISSN: 1975-7220

Effects of diluents on NO_x formation in coflow CH_4/air diffusion flames

Huan Dong*, Yue Zhang, and Zhongzhu Gu*,†**

*School of Energy and Mechanical Engineering, Nanjing Normal University, No.78 Bancang Street, Nanjing 210042, China
**Jiangsu Guoxin Yangzhou Power Generation Co., LTD., Bali Town, Yangzhou 225131, China
(*Received 22 September 2013 • accepted 28 January 2014*)

Abstract−The effect of diluent addition on NO_x formation in a laminar CH_4/air coflow diffusion flame was investigated by numerical simulation with experimental verification. The hydrocarbon fuel stream was diluted with N_2, CO_2, and Ar. The volume fraction of diluents systematically changed from 0.0 to 0.5. The simulation data agree well with the experimental one. The computational results indicate that overall the three diluents reduce the formation of NO and the effects vary from weak to strong in the order: N_2, Ar and CO_2. Differences between the influences of the various diluents are discussed in terms of the thermal, the dilution and the direct chemical effects, respectively. Further, the addition of CO_2 reduces the formation of NO_2, while the addition of N_2 or Ar has little effect on it. However, the formation rate of N_2O increases by each of the added diluents.

Keywords: NO_x, Laminar Diffusion Flame, Diluents

INTRODUCTION

Combustion with diluents added in gaseous fuel is an effective way to reduce emissions of NO_x [1-6]. Essentially, diluted combustion is a specific form of exhaust-gas recirculation combustion, which is of paramount importance in combustion for high fuel efficiency and low pollutant emissions. There have been studies concerning the effects of adding diluents on NO_x formation. An excellent review of the effect of carbon dioxide as an additive on NO_x formation in an ethylene diffusion flame was presented by Liu et al. [7]. Guo et al. [8] studied the effect of hydrogen/reformate gas addition on flame temperature and NO formation in CH_4/air diffusion flames. The effect of diluents such as N_2, CO_2, and He on NO_x formation in H_2/air counterflow flames was investigated by Rørtveit et al. [4]. Park et al. [9] discussed the dilution effect of air stream on flame structure and NO emission characteristic in CH_4/air counterflow diffusion flame. The results of the above studies show that in hydrocarbon diffusion flames, NO, the dominant component of NO_x is mainly formed by the prompt route. When diluents are added to a hydrocarbon diffusion flame, it is expected that the formation of NO by the prompt route can decrease or increase due to the variation in CH radical. On the other hand, the addition of diluents may modify flame temperature and the fraction of free OH, O and H radicals, which may change the formation of NO by the thermal route. Despite some developments in the effects of diluents on NO_x formation for hydrocarbon flames, there are still many important issues that remain unresolved, especially the lack of knowledge on the variation laws and effect mechanisms.

In this paper, laminar coflow diffusion flames are selected as the research object since their properties can be used to analyze combustion in various conditions, and to interpret fundamental physico-chemical mechanisms. Methane is selected as the base fuel because the chemical kinetics of this simple hydrocarbon fuel is relatively well known and its direct relevance to natural gas combustion. Diluents are added to the fuel side. Three diluents with different properties have been studied to ascertain their effects on the formation of NO_x. N_2, CO_2 and Ar have been added as diluents to the fuel side in coflow diffusion flames. While N_2, CO_2 were chosen for their prevalence and potential relevance to recirculation of burned hydrocarbon flue gases, Ar was selected to investigate the influence of its transport coefficients because of its definite lack of involvement in chemistry. The general objective of this study was to increase knowledge of the combustion mechanism controlling NO_x emissions from diluted flames.

EXPERIMENTAL METHODOLOGY

The experiment was conducted in a coflow axisymmetric laminar diffusion flame burner, as shown in Fig. 1. The fuel stream issued from a 10.9-mm-inner-diameter vertical tube, and the oxidant (air) from the annular region between the fuel tube and a 101-mm-diameter concentric tube. Before exiting the annular region the air passed through packed beds of glass beads and porous metal disks, which are conducive to keeping the flame stable. The wall thickness of the fuel tube is 0.96 mm. The base flame is coflow methane/air diffusion flame. During the experiment, the mass flow rates of methane and air were, respectively, 0.141 g/min and 4.724 g/min at room temperature (298 K) and atmosphere pressure. The methane used was analytical grade (99.99% pure).The air used was provided from compressed gas cylinder. A flame enclosure made of flexible steel mesh protects the flame from air movements in the room. The burner was mounted at a positioning platform with nice and repeatable vertical and horizontal movement capability. The concentration of NO in off-gas was measured by handheld gas analyzer (ecom-J2KN made in Germany). The gas analyzer consists of gas flow system and circuitry. Its working principle is like this: gas is sent to the sensor's gas cell from the sampling tube by sampling pump, and the electrical signal which is transformed by the sensor is converted into the

†To whom correspondence should be addressed.
E-mail: guzhongzhu@njnu.edu.cn

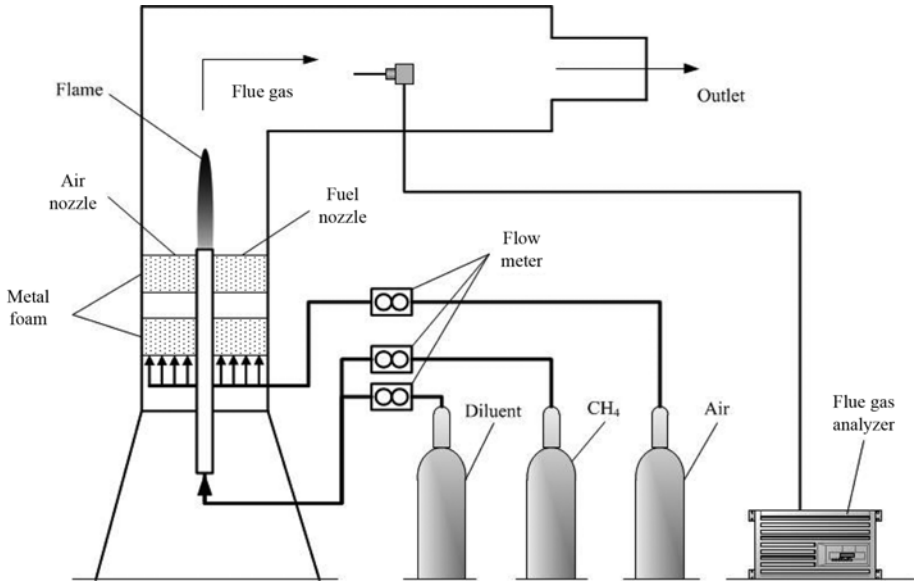

Fig. 1. Schematic diagram of the measurement system.

concentrations of measured gas. Note that limited by the accuracy of the analyzer (±5 ppm) and the low level of NO_2 concentration (<15 ppm), the measurements of NO_2 are not used for the verification of mathematical model, though the gas analyzer is able to also measure NO_2.

NUMERICAL MODEL

The experimental flames above were modeled by numerical simulation. The governing equations for conservation of mass, momentum, energy and gas species mass fractions can be found elsewhere [10]. Low Mach number assumption was adopted. The governing equations were discretized using the finite volume method in axisymmetric cylindrical coordinates. The SIMPLE numerical scheme [11] was used to handle the pressure and velocity coupling. The diffusion terms in the conservation equations were discretized by the central difference method and the convective terms were discretized by the power law method [10]. To speed up the convergence process, the discretized governing equations of gas species were solved in a fully coupled fashion at each control volume [12]. Those of momentum, energy and pressure correction were solved using the tri-diagonal matrix algorithm.

The computational domain covered the region from 0 to 3.0 cm in the radial direction and 0 to 11.0 cm in the axial direction. It was shown that this computational domain was sufficient, and thus the boundary location did not influence the simulation result. The inflow boundary (z=0 cm) corresponded to the region immediately above the fuel nozzle. Totally 160(z)×95(r) non-uniform grids were used in the simulations, with finer grids being placed in the primary reaction zone and near the fuel nozzle exit region. It was checked that the further increase of grid number did not significantly influence the simulation results.

The chemical reaction mechanism used is GRI-Mech 3.0. Though it is reported that GRI 3.0 may lead to an overestimation of prompt-NO_x when the thermal route makes an important contribution to NO_x formation [13], the mechanism could still give reasonable and reliable predications for diffusion flames under most conditions, especially when the prompt route dominates the formation of NO_x [14].

The thermal and transport properties were obtained by using the database of GRI-Mech 3.0 and the algorithms given in [15,16]. The thermal diffusion velocity of H_2 and H was accounted for, while that of other species was ignored. Radiation heat transfer was calculated by the method given by Liu et al. [17].

RESULTS AND DISCUSSION

In all the studied flames, the fuel stream consists of CH_4 and diluents. The fraction of diluents is defined as

$$\alpha_d = \frac{V_d}{V_d + V_{CH_4}} \tag{1}$$

where V_d and V_{CH_4} are the diluent and methane volume flow, respectively.

The NO_x emission is described by both the mole fraction and the emission index, which is defined as the ratio of total formed NO_x to total heat release and calculated as

$$EI_{NO_x} = \frac{V_{FG} M_{NO_x}}{V_{CH_4} M_{CH_4} q_{CH_4} + V_d M_d q_d} \cdot \alpha_{NO_x} \tag{2}$$

where α_{NO_x} is the NO volume fraction, and V_{CH_4}, V_d, V_{FG} is the volume flow of methane, diluent and theoretical dry flue gas, respectively, in normal temperature and pressure. Quantities M_{NO_x}, M_{CH_4} and M_d are, respectively, the NO, methane and diluent molecular weight. Quantities q_{CH_4} and q_d is the methane and diluent heat value. In this study, all the three diluents are incombustible, so the formula can be simplified into

$$EI_{NO_x} = \frac{V_{FG} M_{NO_x}}{V_{CH_4} M_{CH_4} q_{CH_4}} \cdot \alpha_{NO_x} \tag{3}$$

1. Experimental Verification of Mathematical Model

Figs. 2 to 4 display the variations of the NO mole fraction as the diluent fraction α_{N_2}, α_{CO_2} and α_{Ar} change, respectively, and compare

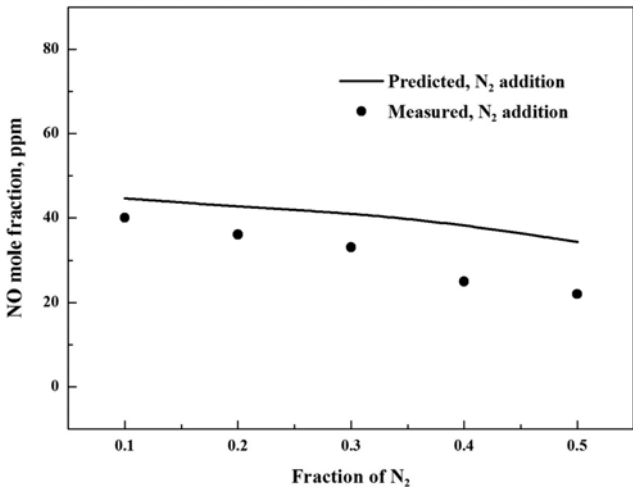

Fig. 2. Variation of NO mole fraction at different N_2 fractions.

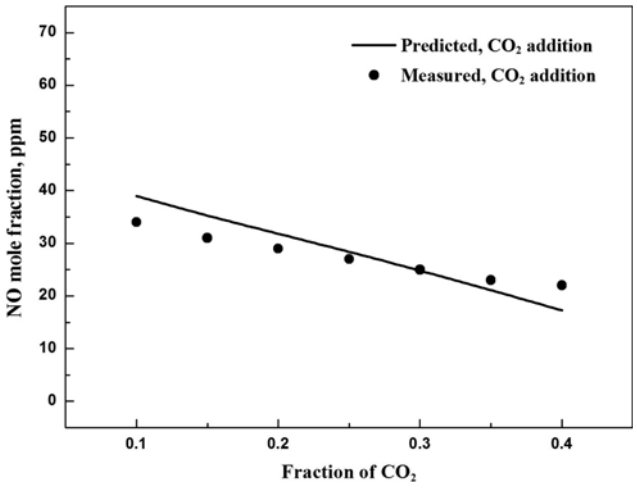

Fig. 3. Variation of NO mole fraction at different CO_2 fractions.

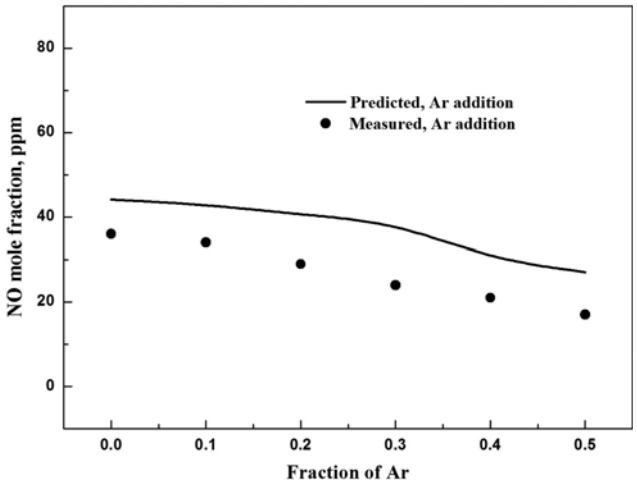

Fig. 4. Variation of NO mole fraction at different Ar fractions.

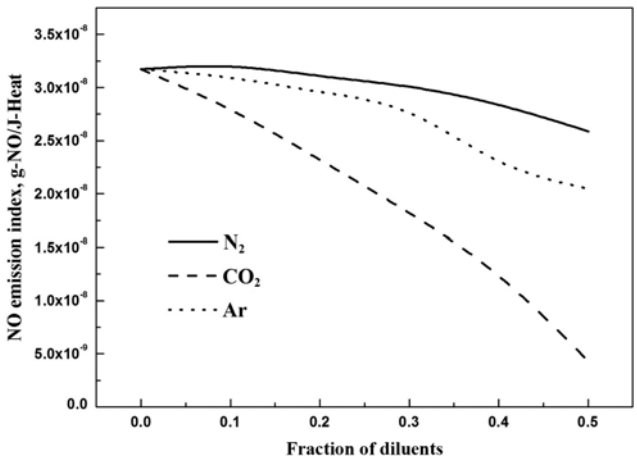

Fig. 5. Variation of NO emission index at different fractions of diluents.

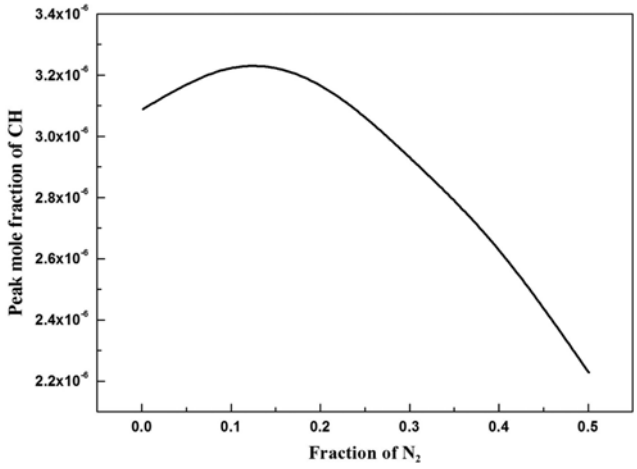

Fig. 6. Variation of peak CH mole fraction at different N_2 fractions.

the experimental and computational results in different diluent conditions. The figures show that the trend of calculation curves agree well with the experiment data, which can prove that the mathematical model is acceptable and can be used to the numerical research on NO_x formation in diluted coflow CH_4/Air diffusion flames.

2. Simulation of NO Formation

The variation of NO emission indexes versus the fractions of different diluents is depicted in Fig. 5. When diluent is added to the fuel, NO formation can be affected owing to the thermal, the dilution, and the direct chemical reaction effect. The dilution and the chemical reaction effect are analyzed simultaneously, for the N_2, CO_2 and Ar dilution, respectively. Meanwhile, the thermal effect will be discussed separately later.

Considering the curve of N_2, as α_{N_2} increases from 0.0 to 0.1, the NO emission index increases, then the NO emission index decreases as α_{N_2} increases from 0.1 to 0.5. The variation above can be explained by the mechanism of NO formation. The previous research proves that the method to identify the mechanism of NO formation in a flame should not be based on how NO is finally formed, but on how molecular nitrogen is originally converted to atomic nitrogen or element nitrogen [17]. In the CH_4/air diffusion flame, the formation of atomic nitrogen comes from the paths N_2 (+CH) →HCN→NCO→NH→N and N_2 (+CH) →N, which is the typical prompt route nitrogen conversion. Therefore, as α_{N_2} increases from 0.0 to 0.1, the

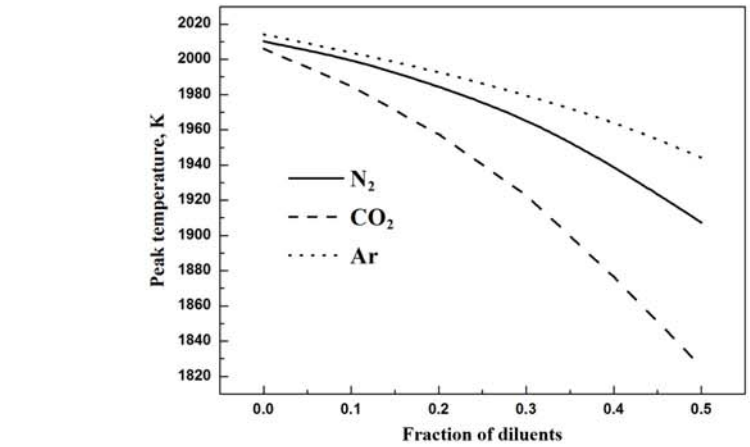

(a)

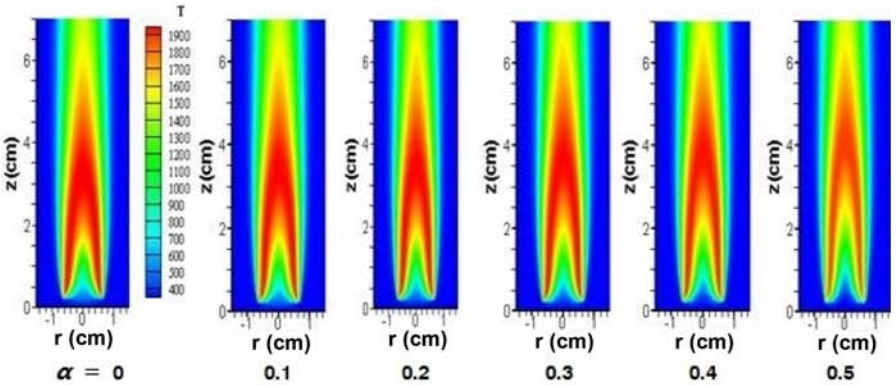

(b)

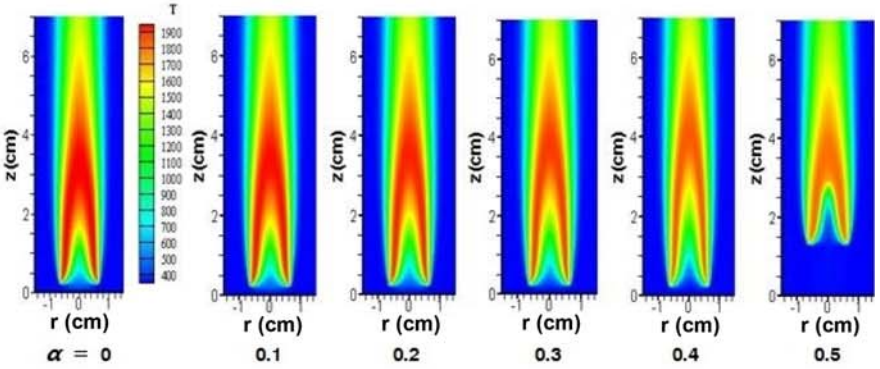

(c)

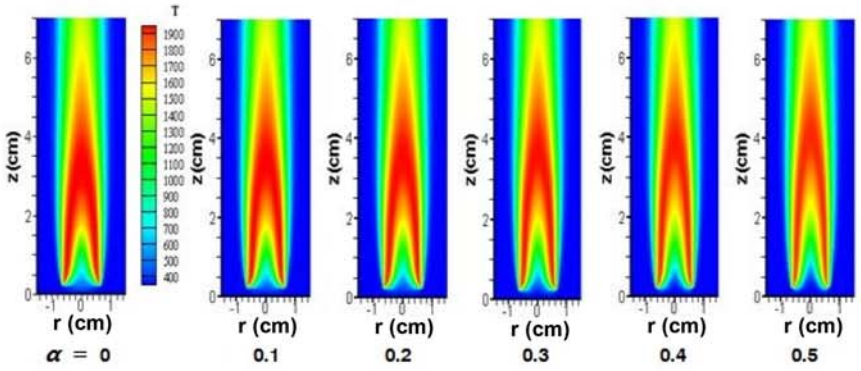

(d)

Fig. 7. Variation of temperature at different fractions of diluents.
(a) Variation of peak temperature, (b) The temperature distributions with the N_2 fraction from 0 to 0.5, (c) The temperature distributions with the CO_2 fraction from 0 to 0.5, (d) The temperature distributions with the Ar fraction from 0 to 0.5

maximum concentration of CH radical increases, as shown in Fig. 6, which prompts the above paths. As the α_{N_2} increases from 0.1 to 0.5, the maximum concentration of CH radical decreases, which reduces the concentration of atomic nitrogen. A similar description of an increasing NO emission result from a higher CH radical concentration in a lightly diluted flame can be found in other research [18]. Those are the dilution and chemical effects by N_2 dilution.

For the flame with CO_2 added, the dilution effect lowers the maximum concentrations of H, O, and OH radicals, as shown in Fig. 8. The chemical effects of CO_2 addition mainly include the reactions $CO_2+H \rightarrow CO+OH$ and $CO_2+CH \rightarrow CO+HCO$, which can reduce the concentrations of H and CH radicals. According to the general process of methane oxidation described in the research [19], CH_3 is formed through the reaction of CH_4 with H, O and OH, and reacts with H to form CH_2 and CH, hence the concentrations of H, O, and OH have influences on the formation of CH, which are extremely involved in the formation of NO as referred above. Both the dilution and chemical effects of CO_2 addition lead to reductions of CH by inhibiting O, OH or H, and the chemical effect inhibits the formation of CH directly as well.

As an inert diluent, Ar participates in no chemical reactions. Therefore, the reduction of NO formation caused by Ar added can be covered by the results of dilution and thermal effects. Similar to the dilution effect of CO_2, the one of Ar lowers the maximum concentrations of the O, H, and OH radicals (Fig. 9) and thus decrease the formation of NO.

The thermal effects of diluents decrease the flame peak temperatures, and are relevant to the diluent heat capacities [20]. CO_2 has a specific heat at constant pressure (C_p) up to 37.06, N_2 29.19, and Ar 20.77 ($J*mol^{-1}*K^{-1}$, STP). A higher heat capacity leads to a stronger decline of flame peak temperature, as shown in Fig. 7. Since CO_2 has the highest C_p which causes the most heat loss among the three diluents, the largest decline rate of temperature was found in the flame by CO_2 dilution and results in a rapid reduction of NO emission index (Fig. 5). For the thermal effects of N_2 and Ar, although N_2 has the higher C_p and faster lowers the flame peak temperature, it gives a weaker decline of NO emission than Ar. It is because N_2 directly takes part in the chemical reactions and thus contributes to NO formation, as discussed above.

3. Simulation of NO_2 Formation

Fig. 10 shows the variation of NO_2 emission index when the dil-

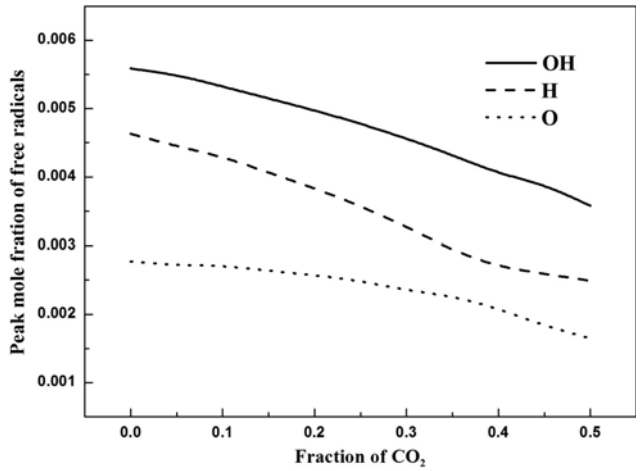

Fig. 8. Variations of peak H, O and OH mole fractions at different CO_2 fractions.

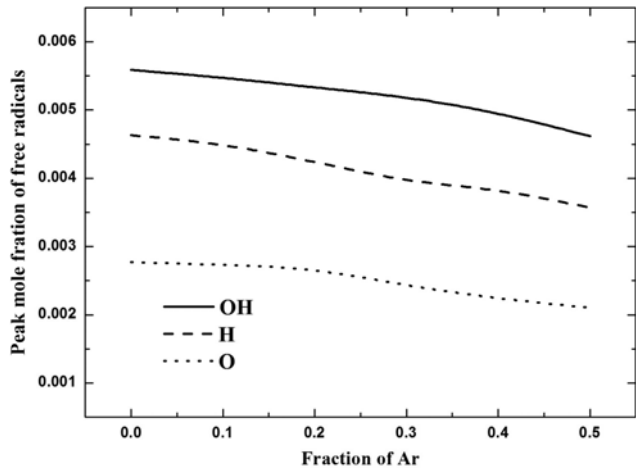

Fig. 9. Variations of peak H, O and OH mole fractions at different Ar fractions.

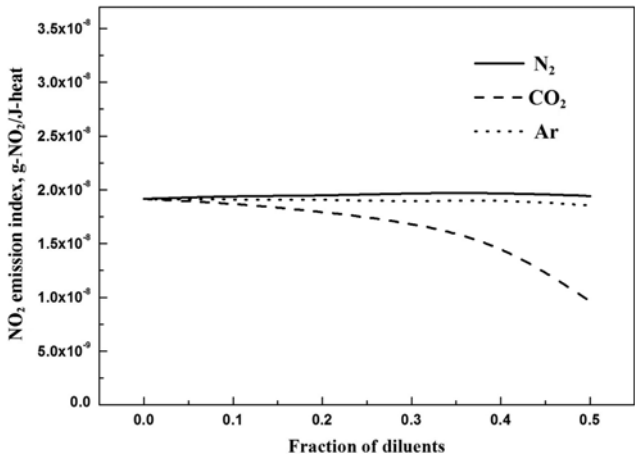

Fig. 10. Variation of NO_2 emission index at different fractions of diluents.

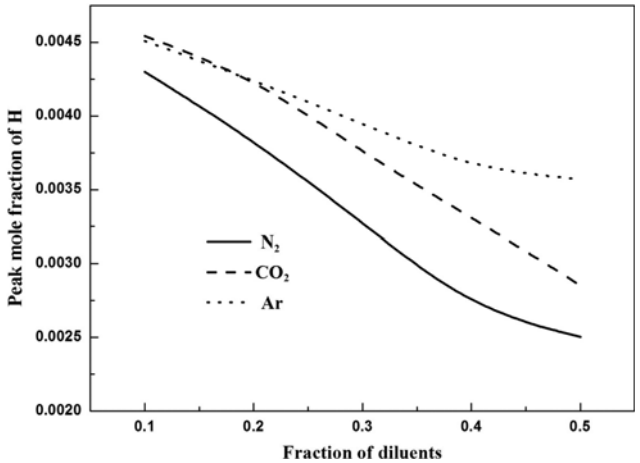

Fig. 11. Variation of peak H mole fraction at different fractions of diluents.

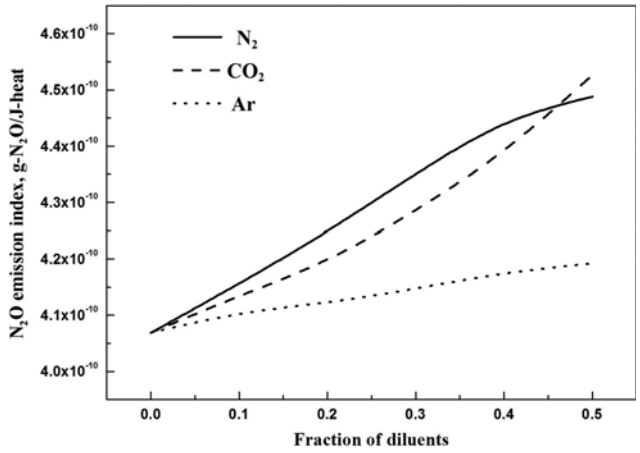

Fig. 12. Variation of N_2O emission index at different fractions of diluents.

uents are added. It is illustrated that the addition of CO_2 decreases the formation of NO_2, while the addition of N_2 or Ar has little effect on it. A sensitivity analysis [21] pointed out that the formation and destruction of NO_2 are, respectively, $HO_2+NO=NO_2+OH$ and $NO_2+H=NO+OH$. As discussed before, the addition of diluents reduces the formation of NO, thereby leading to decrease of the formation rate of NO_2. As shown in Fig. 11, the addition of diluents reduces the fraction of H, trending to decrease the destruction rate of NO_2. As the superposition of these two conflicting trends, the formation of NO_2 is slightly reduced or almost constant.

4. Simulation of N_2O Formation

Fig. 12 displays the variation of N_2O emission index with the addition of diluents. It is indicated that the addition of CO_2 or N_2 rapidly increases the formation of N_2O, while the addition of Ar slightly increases it. A similar variation was found in the biomass combustion experiments performed by Houshfar [22], where the N_2O concentration increases with primary excess air ratio and in general the favorable conditions for NO_x reduction result in more N_2O formation. The main destruction reactions of N_2O are $N_2O+M=N_2+O+M$ and $N_2O+H=N_2+OH$. When the diluents are added, the reductions of the flame peak temperature and H concentration as shown in Fig. 7 and Fig. 11, inhibit the destruction of N_2O, resulting in the increase of its emission index.

CONCLUSIONS

(a) The effect of diluent addition to fuel stream on NO_x formation in CH_4/air laminar coflow diffusion flame was studied by simulations and experimental verification with the diluents N_2, CO_2 and Ar added, respectively.

(b) The simulations successfully reproduced the experimental phenomenon, which proved that the model is reliable.

(c) The simulation results indicate that all of the three diluents can reduce the formation of NO to varying degrees. For flames with N_2 added, NO emission index has an exceedingly slight rise when $\alpha_{N_2}<0.1$ and obviously decreases after α_{N_2} goes upon 0.1. The additions of CO_2 or Ar result in a monotonic reduction of the NO emission index. Among the three diluents CO_2 is the most efficient, with Ar following behind. The addition of CO_2 and N_2 reduces NO formation through the thermal, dilution and direct chemical effects, while Ar suppresses the NO formation through the thermal and the dilution effects only.

(d) The addition of CO_2 decreases the formation of NO_2, while the addition of N_2 or Ar has little effect on it.

(e) Addition of each diluent among CO_2, N_2 and Ar increases the formation rate of N_2O to varying degrees.

ACKNOWLEDGEMENTS

This research was financially supported by the research prospective project of Jiangsu provincial science and technology department (No. BY 2013001-02) and industrialization project of Jiangsu provincial education department (No. JHB2012-15).

REFERENCES

1. C. Lee and H. G. Kil, *Korean J. Chem. Eng.*, **26**, 862 (2009).
2. J. J. Feese and S. R. Turns, *Combust. Flame*, **113**, 66 (1998).
3. S. C. Li and F. A. Williams, *Combust. Flame*, **118**, 399 (1999).
4. G. J. Rørtveit, J. E. Hustad, S. C. Li and F. A. Williams, *Combust. Flame*, **130**, 48 (2002).
5. F. Liu, H. Guo, G. J. Smallwood and Ö. L. Gülder, *Combust. Flame*, **125**, 778 (2001).
6. A. Beltrame, P. Porshnev, W. Merchan-Merchan, A. Saveliev, A. Fridman, L. A. Kennedy, O. Petrova, S. Zhdanok, F. Amouri and O. Charon, *Combust. Flame*, **124**, 295 (2001).
7. F. Liu, H. Guo, G. J. Smallwood and Ö. L. Gülder, *Combust. Flame*, **125**, 778 (2001).
8. H. Guo and W. S. Neill, *Combust. Flame*, **156**, 477 (2009).
9. J. Park, S. G. Kim, K. M. Lee and T. K. Kim, *Int. J. Energy Res.*, **26**, 1141 (2002).
10. H. Guo, F. Liu, G. J. Smallwood and Ö. L. Gülder, *Combust. Flame*, **145**, 324 (2006).
11. S. V. Patankar, *Numerical heat transfer and fluid flow*, Hemisphere, New York (1980).
12. Z. Liu, C. Liao, C. Liu and S. McCormick, in *AIAA, Aerospace Sciences Meeting and Exhibit*, 33rd, Reno (1995).
13. T. Shimizu, F. A. Williams and A. Frassoldati. *J. Propul. Power*, **21**, 1019 (2005).
14. S. V. Naik and N. M. Laurendeau, *Combust. Sci. Technol.*, **176**, 1809 (2004).
15. R. J. Kee, J. Warnatz and J. A. Miller, *NTIS*, Springfield (1983).
16. R. J. Kee, J. A. Miller and T. H. Jefferson, *CHEMKIN: A general-purpose, problem-independent, transportable, FORTRAN chemical kinetics code package*, Sandia Labs., Livermore (1980).
17. F. Liu, H. Guo and G. S. Smallwood, *Combust. Flame*, **138**, 136 (2004).
18. S. Göke and C. O. Paschereit, *J. Propul. Power*, **29**, 249 (2013).
19. H. Guo, W. Neill and G. J. Smallwood, *Proceedings of IMECE2006*, Chicago (2006).
20. A. Rangrazi, H. Niazmand and H. M. Heravi, *Korean J. Chem. Eng.*, **30**, 1588 (2013).
21. H. Guo, G. J. Smallwood and Ö. L. Gülder, *P. Combust. Inst.*, **31**, 1197 (2007).
22. E. Houshfar, T. Løvås and Ø. Skreiberg, *Energies*, **5**, 270 (2012).